ADDENDUM

Corrigendum and Addendum: Helium flux effects on bubble growth and surface morphology in plasma-facing tungsten from large-scale molecular dynamics simulations (2019 *Nucl. Fusion* 59 066035)

To cite this article: Karl D. Hammond *et al* 2020 *Nucl. Fusion* **60** 129401

IOP Publishing | International Atomic Energy Agency Nuclear Fusion

Nucl. Fusion **60** (2020) 129401 (8pp) https://doi.org/10.1088/1741-4326/abb2d3

Corrigendum and Addendum: Helium flux effects on bubble growth and surface morphology in plasma-facing tungsten from large-scale molecular dynamics simulations (2019 *Nucl. Fusion* 59 066035)

Karl D. Hammond[1,2], Brandon F. Lee[1], Ian V. Naeger[1], Wathsala Widanagamaachchi[3,a], Li-Ta Lo[4], Dimitrios Maroudas[5] and Brian D. Wirth[6,7]

[1] Department of Chemical Engineering, University of Missouri, Columbia, MO 65211, United States of America
[2] Nuclear Engineering Program, University of Missouri, Columbia, MO 65211, United States of America
[3] Scientific Computing and Imaging Institute, University of Utah, Salt Lake City, UT 84122, United States of America
[4] Data Science at Scale Team, Los Alamos National Laboratory, Los Alamos, NM 87545, United States of America
[5] Department of Chemical Engineering, University of Massachusetts, Amherst, MA 01003, United States of America
[6] Department of Nuclear Engineering, University of Tennessee, Knoxville, TN 37996, United States of America
[7] Fusion and Materials for Nuclear Systems Division, Oak Ridge National Laboratory, Oak Ridge, TN 37831, United States of America

E-mail: hammondkd@missouri.edu

Received 30 June 2020, revised 2 August 2020
Accepted for publication 26 August 2020
Published 7 October 2020

Abstract

Two of the simulations discussed in a prior article (Hammond *et al* 2019 *Nucl. Fusion* **59** 066035) were affected by a simulation glitch. We repeated the affected calculations and discuss them here. The overall conclusions are essentially unchanged, though the details are different. In particular, observations that we referred to as 'concerted bursting' were caused primarily by non-physical heating and cooling applied by the thermostat after most atoms' velocities were deleted (for reasons that are not known for certain). The phenomenon of one bubble bursting and causing another nearby bubble to burst does exist, though its effects are much less spectacular in the absence of non-physical driving forces. The observation of an interconnected network of sub-surface cavities formed by burst bubbles is real, and the observation of holes on the surface 1–2 nm in diameter is also confirmed.

Keywords: tungsten, helium, molecular dynamics, fuzz, bubble

(Some figures may appear in colour only in the online journal)

[a] Present affiliation: Internal Medicine, University of Utah, Salt Lake City, UT 84122, United States of America

1. Corrigenda

In a prior article [1], we discussed molecular dynamics (MD) simulations of helium in plasma-facing tungsten at four different values of the incident helium flux spanning four orders of magnitude. In particular, we discussed a peculiar phenomenon: there were brief intervals of time in two different simulations in which several large bubbles burst simultaneously, resulting in significant, rapid surface rearrangement. We speculated that this phenomenon, which we dubbed 'concerted bubble bursting,' could cause significant surface evolution at longer times. We sought to study this phenomenon in more detail by repeating portions of the calculations with shorter intervals between snapshots.

In the course of repeating the affected portions of the calculations—a computationally-intensive process involving several months of wall time—we noticed that the kinetic energy had dropped essentially to zero in the output just before these 'concerted' bursting events and rapid surface deformations occurred. The thermostat would then attempt to adjust the temperature of the entire system. In all cases of this glitch we observed, the vast majority of the atoms started 'cold' and had significant forces exerted on them by the thermostat. Like most controllers, the step response of the thermostat produced significant overshoot in temperature, and it was during these overshoot periods—which were shorter in time than the output of atomic positions and could only be discerned by parsing the thermodynamic output—that the surface deformations occurred. Unfortunately, this was not obvious unless one looked through the lines of output one-by-one, and was not caught prior to publication.

This glitch occurs very infrequently—we hypothesize that it is linked to a rare event, such as insertion of helium atoms inside a bubble in such a manner that it causes high forces, and thus an equally sudden response from the thermostat once those forces act. An attempt is made to move any helium atoms that are inserted too close to other atoms away by minimizing the energy with respect to the position of the inserted atom, but this mechanism would not catch an atom that was inserted in close proximity to a group of helium atoms surrounding it, none of which could move until dynamics resumed. The result would be that several helium atoms shoot away with high kinetic energy, which the thermostat reacts to by cooling everything else; those atoms then escaped the simulation, and the thermostat reacted by heating the entire system back up again, producing overshoot that caused near-surface bubbles throughout the system to deform and/or burst.

This glitch has also occurred with less spectacular results in a couple of instances—for example, it is responsible for the sudden drop in retention at 4.5793 μs in the sixth figure of one of our previous papers on this subject [2]. However, in that case, the affected bubbles were very near the surface and the resulting trajectory was not strongly affected.

We have repeated the simulation involved in producing the first figure, corresponding to system E in the second table of the original article. The only affected snapshot in the figure was at 2.5 μs, corresponding to Figures 1(*e*), (*j*), (*o*), (*t*), and (*y*). The results of the repeated simulation are in Figure 1. This figure should be interpreted as a corrigendum to the first figure of the original article [1].

The other affected results were those depicted in the third, ninth, tenth, eleventh, and twelfth figures in the original paper, which show data from system B in the second table in the orginal article [1]. That simulation experienced a similar glitch—multiple times—in which the velocities of most if not all atoms were deleted, causing subsequent overheating by the thermostat. Figure 2 shows a reproduction of the third figure of the original paper; the only change is the red lines in part (*a*). Figure 3 shows a similar reproduction of the ninth figure of the original paper, with the red and dark green lines updated in both parts. Figure 4 is a re-plotting of the tenth figure of the original paper, with the red and dark green lines updated in both parts and some additional results included where appopriate for the other plots.

Finally, figure 5 is a full reproduction of the eleventh Figure in the original paper. Only panes (*a*) through (*d*) are in the original; the rest have been re-generated. It should be noted that the same relatively rapid changes in the surface morphology, such as between figures 5(*i*) and 5(*k*), are present. These snapshots are taken less than 30 ns apart, but they show the opening of several large holes in the surface and the widening of others. We also see several surface features begin to 'fill in' over time, presumably as bubbles on either side or below the voids push dislocations into the voids, sealing them or partially filling them in.

It is not clear why these 'glitches' occurred or how reproducible they are. As discussed earlier, we currently believe that they are related to rare events, such as insertion of helium atoms very close to other helium atoms (particularly those in bubbles), combined with the use of a Nosé–Hoover chain thermostat. Simulations experiencing this glitch were run with the 13Aug2013 'pull' of LAMMPS, so it may be associated with a bug in the software that has since been fixed, but we cannot say definitively that this phenomenon does not exist in later versions. If we are correct that this glitch occurs because of helium insertion in bubbles compounded by the thermostat, then it is unlikely that other LAMMPS users will experience similar problems unless they are also using similar insertion algorithms. It should be emphasized that this issue is extremely rare: the phenomenon has been observed less than ten times in over 200 million CPU-hours.

2. Additional results and discussion

The only figure of the original paper that needs to be significantly re-examined in light of this glitch is the twelfth figure, which we now recognize to be non-physical. However, the idea that more than one bubble can burst simultaneously is correct, though the event is less spectacular than we previously reported.

An example of a bubble bursting that causes a nearby bubble to burst is shown in figure 6. It should be noted that the simulation in figure 6 is not the only observation we made with this initial condition: repeating this simulation four times with no helium insertions and with no variables changed resulted

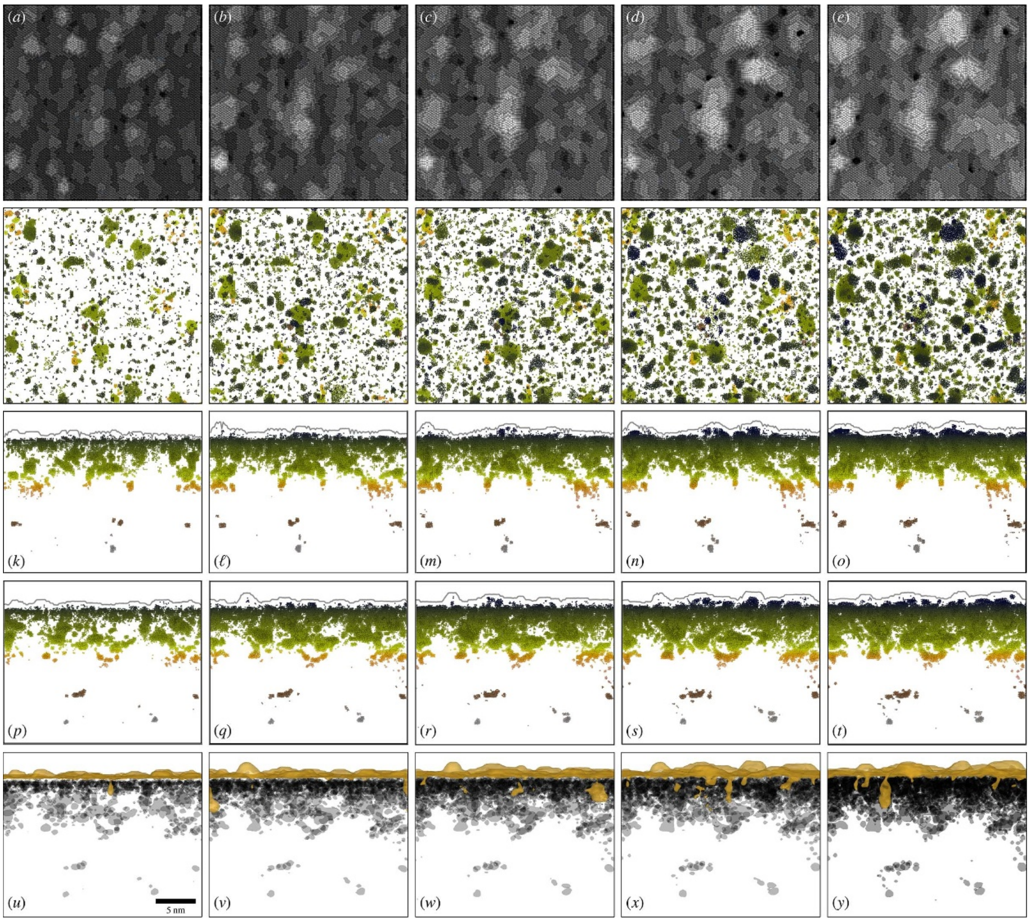

Figure 1. Prototypical surface features on the (0 1 1) surface (*a*)–(*e*); corresponding helium locations shaded by depth (*f*)–(*j*); views of helium atoms projected onto the ($\bar{1}$ 0 0) plane (*k*)–(*o*) and the (0 $\bar{1}$ 1) plane (*p*)–(*t*); and alternative visualizations (projected onto the (0 $\bar{1}$ 1) plane) showing helium atoms, voids, and the surface contour (*u*)–(*y*) for a (0 1 1) surface exposed to helium plasma at a nominal flux (excluding reflected atoms) of 1.60×10^{26} m^{-2} s^{-1}. Times and corresponding fluences are 0.5 μs and 8.02×10^{19} m^{-2}, 1.0 μs and 1.60×10^{20} m^{-2}, 1.5 μs and 2.41×10^{20} m^{-2}, 2.0 μs and 3.21×10^{20} m^{-2}, and 2.5 μs and 4.01×10^{20} m^{-2}. Labels (*f*) through (*j*) are omitted so as not to obscure helium atoms. Surface features in (*a*)–(*e*) are shaded by height, with a linear grayscale between −0.5 nm (black) and +2.0 nm (white) with 50% ambient occlusion in OVITO [3]. Helium atoms in (*f*)–(*t*) are color-coded by depth beneath the original tungsten surface. The gray lines in (*k*)–(*t*) are a projection of the highest point on the surface onto the plane (surface profile). Helium clusters and bubbles in (*u*)–(*y*) are colored black (opacity 15%) and empty spaces/surfaces are colored gold (opacity 50%). *The only changes from the original are images (e), (j), (o), (t), and (y).*

in three simulations in which concerted bursting was observed and one simulation in which the first bubble bursts but the membrane is able to 'flex' enough to hold the pressure of the second bubble in place. In this particular instance, it means the forces on each atom are so close to the local yield stress that random fluctuations (such as those caused by round-off errors or fluctuations from the thermostat) are enough in some cases to dislodge the tungsten membrane but are insufficient in others.

Large bursting events that vented significant fractions of the helium inventory were also observed, but the mechanism is different than previously reported. In System B, the largest bubble observed contained about 11,800 helium atoms, thus venting about 20% of the helium inventory when it burst. Three other bubbles of similar size (11,500 atoms, 8,400 atoms, and 7,900 atoms) were observed in the simulations of System B, with each bubble being roughly 10 nm across (which is approximately the upper-end diameter of experimentally-observed cavities). The venting time (i.e. the interval between the escape of the first helium atom to the time the last helium atom is released) of these bubbles ranged from 237.5 ps to 1330 ps. While these bubbles were comparable in size with the lateral dimensions of the supercell, they did not join with themselves across periodic boundaries, so we can be reasonably confident that finite-size effects did not drastically alter their behavior. Each of these bubbles grew to (relatively) large sizes through the inflation–collapse cycles of other bubbles—that is, by absorbing nearby bubbles as the primary bubble expands, bursting and venting its contents to the plasma, then sealing and refilling with helium—with the cavities usually expanding on each cycle. In fact, two of these large bubbles formed in the same cavity at different times. It should also be noted that these large bubbles all formed and burst before reaching a fluence of 1.2×10^{21} m^{-2}, corresponding to about 240 ns of simulated time. This process was certainly accelerated by several orders of magnitude by the high

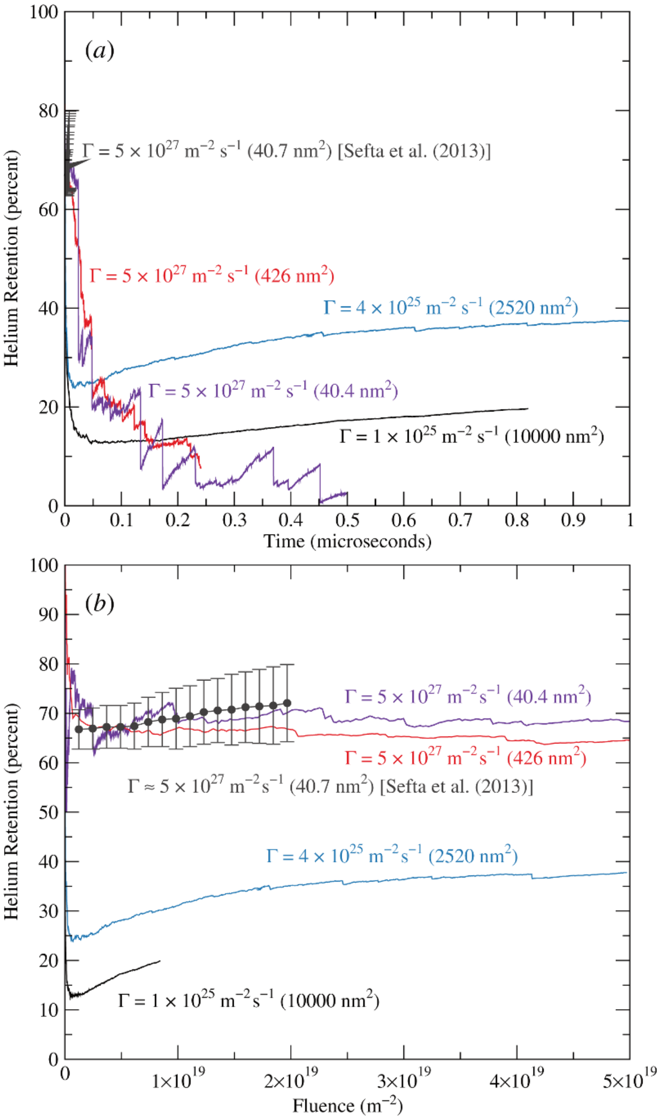

Figure 2. [originally figure 3] Helium retention as a function of (*a*) time and (*b*) fluence for various fluxes of impinging helium on W(001) surfaces. The area of the plasma-facing surface is given in parentheses as a rough reminder of simulation supercell size. Note that the sudden drops in retention, visible only in the $\Gamma \sim 10^{27}\ \mathrm{m}^{-2}\,\mathrm{s}^{-1}$ simulations at this time scale, correspond to the bursting of bubbles—the drops are more pronounced for the smallest simulation supercell (36.6 nm^2 area) compared to the second smallest one (426 nm^2). Included for reference are data at 1200 K from Sefta *et al* [4] (dark gray, with error bars). The data at $\Gamma = 4\times10^{25}\ \mathrm{m}^{-2}\,\mathrm{s}^{-1}$ are discussed in [2]. *The only change from the original figure is the red line in (a) after t = 0.07771* µs.

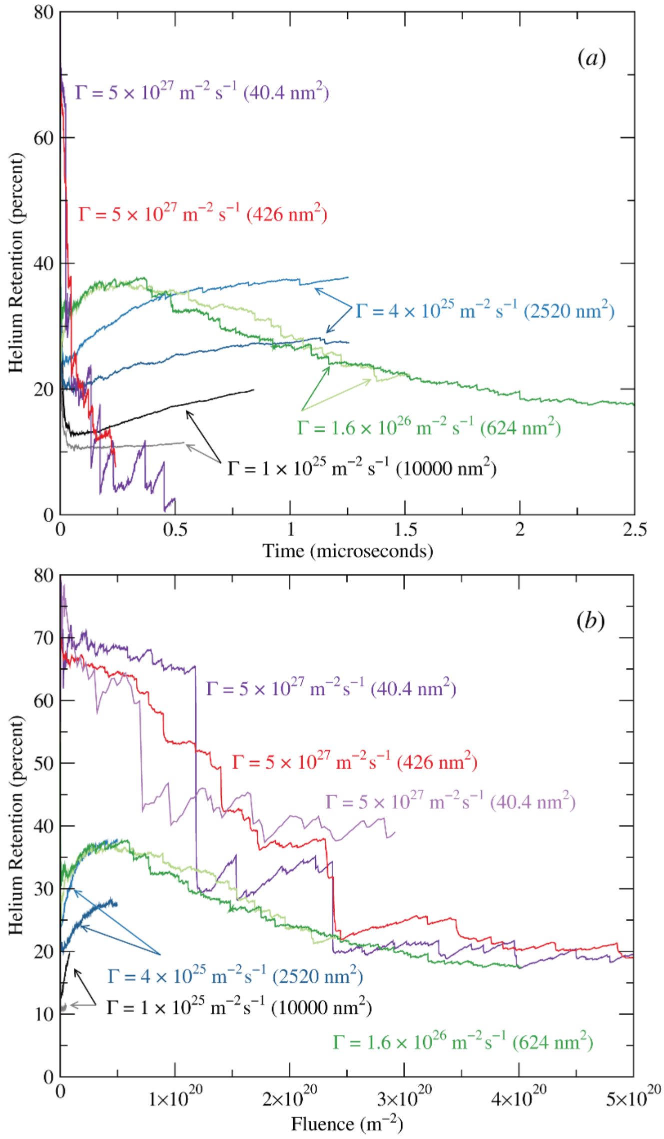

Figure 3. [originally figure 9] Helium retention for various fluxes of impinging helium on W{001} and W{011} surfaces as a function of (*a*) time and (*b*) fluence, similar to figure 2 except at much longer times (at which bubble bursting is more evident).
Note that retention invariably reaches a maximum prior to $\Phi \approx 6\times10^{19}\ \mathrm{m}^{-2}$; this is the onset of bubble bursting, though most bubbles that burst—particularly in the simulations with large supercells—are small, meaning large drops in retention are not visible in the plot. At high fluence, however, bubbles burst that are large enough that they contain a relatively high fraction of the total helium implanted into the system, resulting in an abrupt drop in retention. *The only changes from the original are the red line after t = 0.07771* µs ($\Phi = 3.835\times10^{20}\ \mathrm{m}^{-2}$) *and the dark green line after t = 2.242* µs ($\Phi = 3.594\times10^{20}\ \mathrm{m}^{-2}$).

flux used in the simulation, but this indicates that any bubbles that form in experiments have likely burst and re-filled many, many times.

The observation that bubbles expand by continually filling and bursting is consistent with observations by Doerner and coworkers [5] that fuzz formed under pure ^{4}He plasma followed by 30 min of 25% ^{3}He had similar isotopic ratios to fuzz formed under 25% ^{3}He without pure ^{4}He plasma. The explanation of their results based on our work here—which is admittedly reading a fair amount into our results, given the many orders of magnitude differences in flux and fluence and the drastically different spatial and temporal scales—is that bubbles in real PFCs likely burst and re-fill with helium multiple times, perhaps thousands of times, meaning that the most recent helium plasma composition would largely determine the composition of the helium present in bubbles in the fuzz.

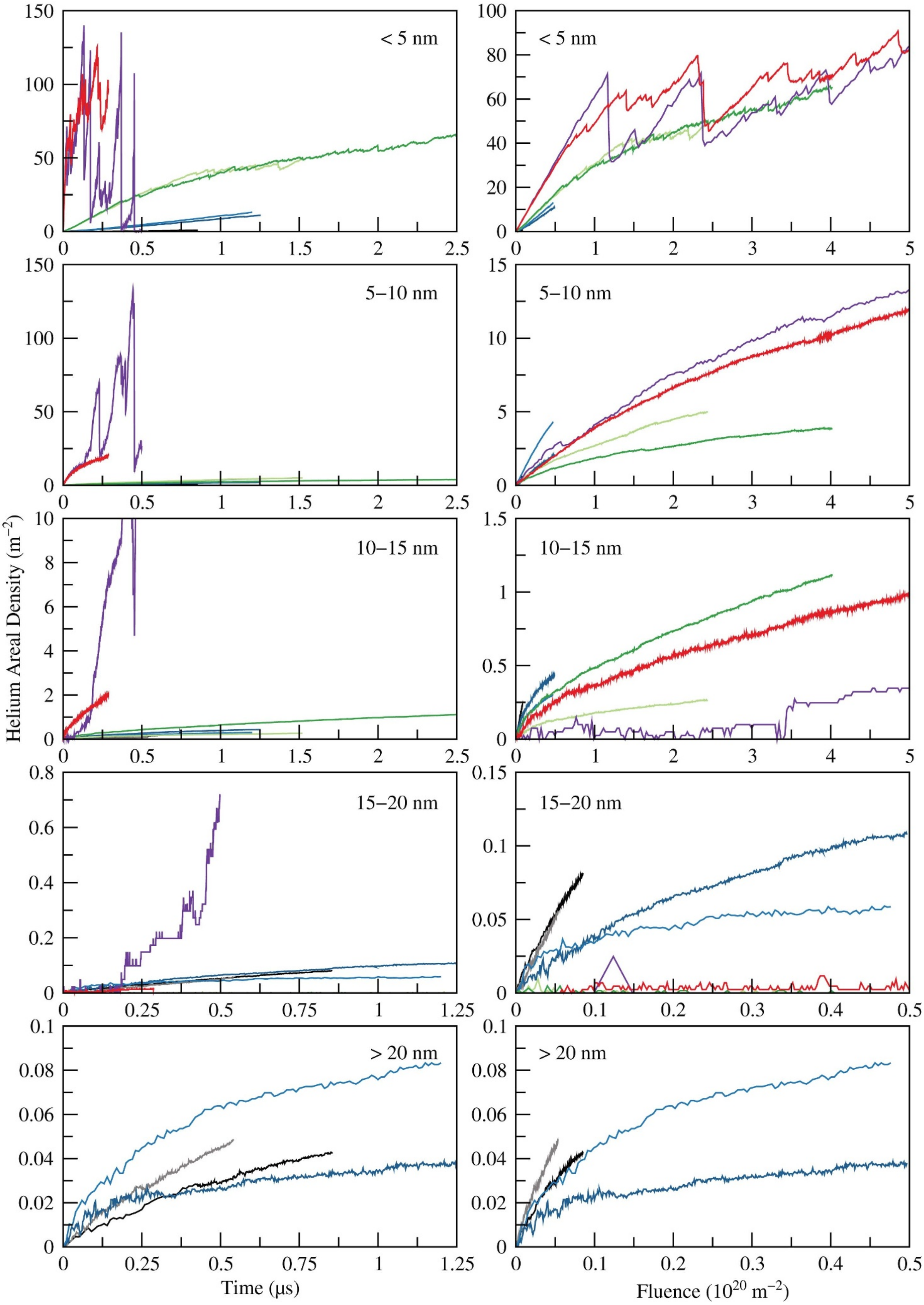

Figure 4. [originally figure 10] Areal density of helium present in each supercell at various depths (5 nm thick layers), using the same color scheme as shown in Figure 3, as a function of time (left) and fluence (right). The vertical and horizontal axes are not all the same, so as to show more clearly the values involved. *The only changes from the original are the red line after t = 0.07771* µs ($\Phi = 3.835 \times 10^{20}$ m^{-2}) *and the dark green line after t = 2.242* µs ($\Phi = 3.594 \times 10^{20}$ m^{-2}).

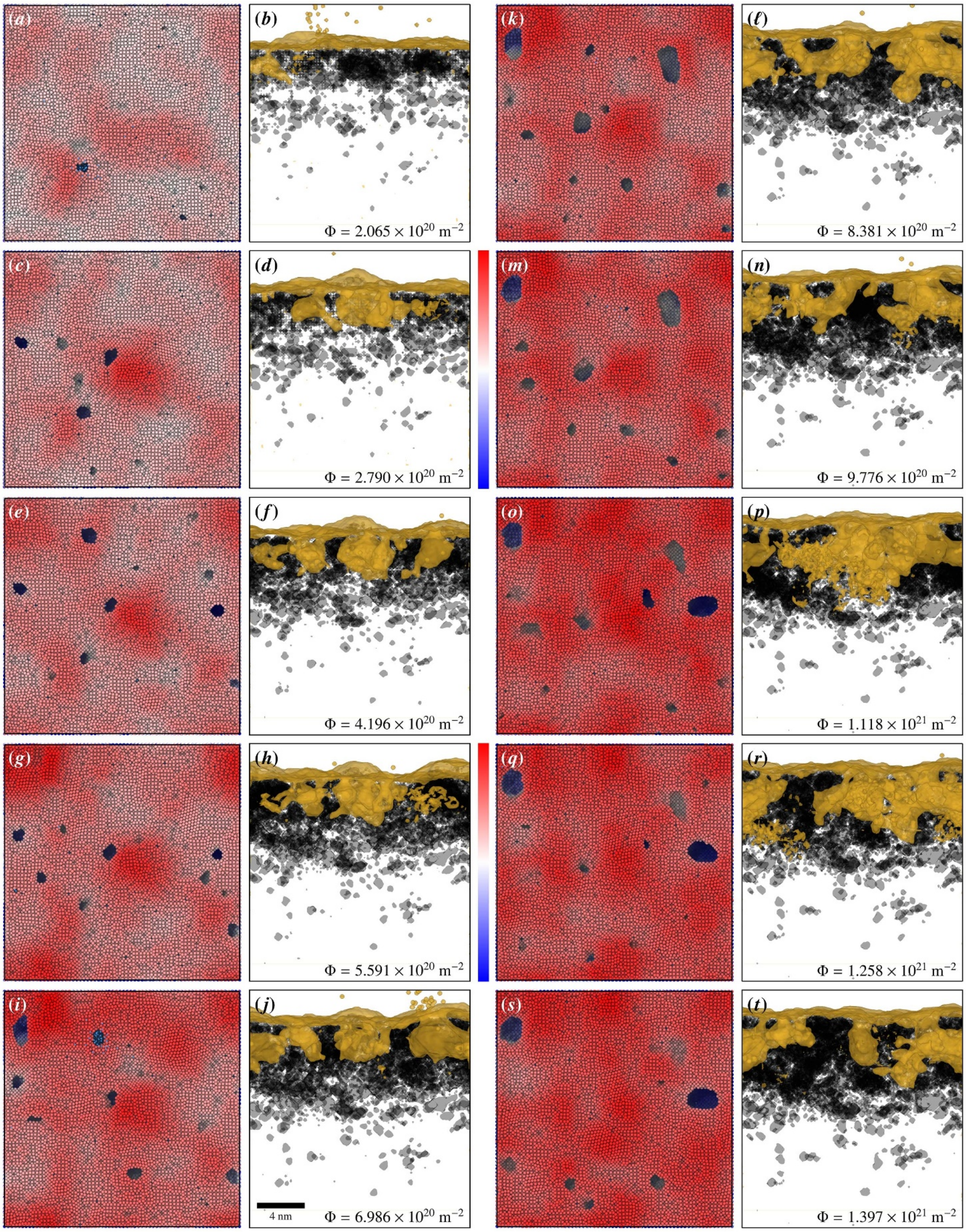

Figure 5. [originally figure 11] Visualization of a sequence of configurations generated in long-time simulations of tungsten W(001) surfaces exposed to 100 eV helium plasma up to a fluence $\Phi \sim 10^{21}$ m^{-2}. The flux is $\Gamma = 4.94 \times 10^{27}$ m^{-2} s^{-1}. The snapshots are taken at $t_{a,b} = 28.50$ ns, $t_{c,d} = 56.53$ ns, $t_{e,f} = 85.03$ ns, $t_{g,h} = 113.29$ ns, $t_{i,j} = 141.55$ ns, $t_{k,\ell} = 169.81$ ns, $t_{m,n} = 198.08$ ns, $t_{o,p} = 226.58$ ns, $t_{q,r} = 254.84$ ns and $t_{s,t} = 283.10$ ns since the onset of plasma exposure. The surfaces on the left-hand images are shaded using a blue–white–red scale from 3.5 nm below the original, pre-plasma-exposure surface (blue) to the original surface (white) to 3.5 nm above the original surface (red), as shown by the color gradient placed between images (*d*) and (*m*) as well as between (*h*) and (*q*); these images also show 30% ambient occlusion as defined in OVITO [3]. The side views $(b, d, f, \ldots)$ are visualizations showing helium bubbles (black) and surfaces/voids (gold). It should be noted that the gold blobs above the surface are helium atoms, not tungsten atoms, in these images. *Images (a)–(d) are the same as in the original.*

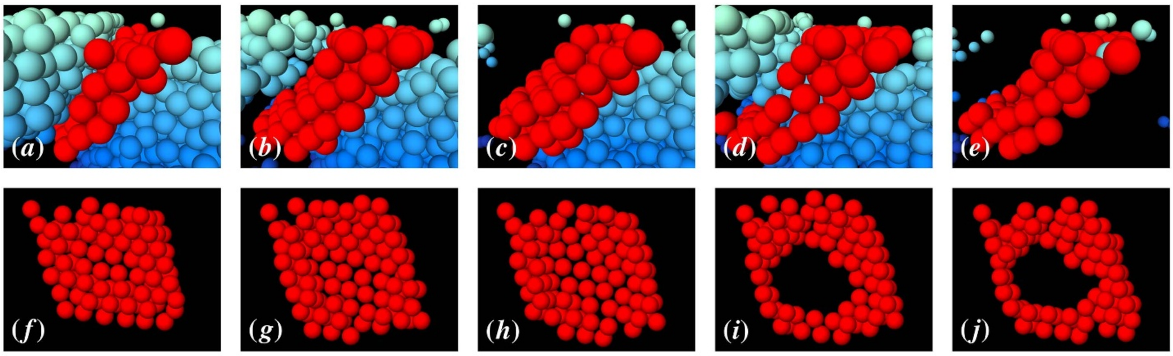

Figure 6. Snapshots of two bubbles during a sequence of bubble bursting events. (*a*) and (*b*): helium (blue/green colors) in both bubbles with a tungsten (red) mebrane separating them. (*c*): bubble on the left has burst; (*d*) membrane bursts, allowing helium from the bubble on the right to vent through the void; (*e*) bubbles after bursting. Images (*f*)–(*j*) are the same images with helium atoms hidden and as viewed from the bubble farthest from the plasma, looking through the membrane into the other bubble in the plasma-facing direction. It should be noted that the membrane between the two bubbles is only one or two tungsten atoms thick.

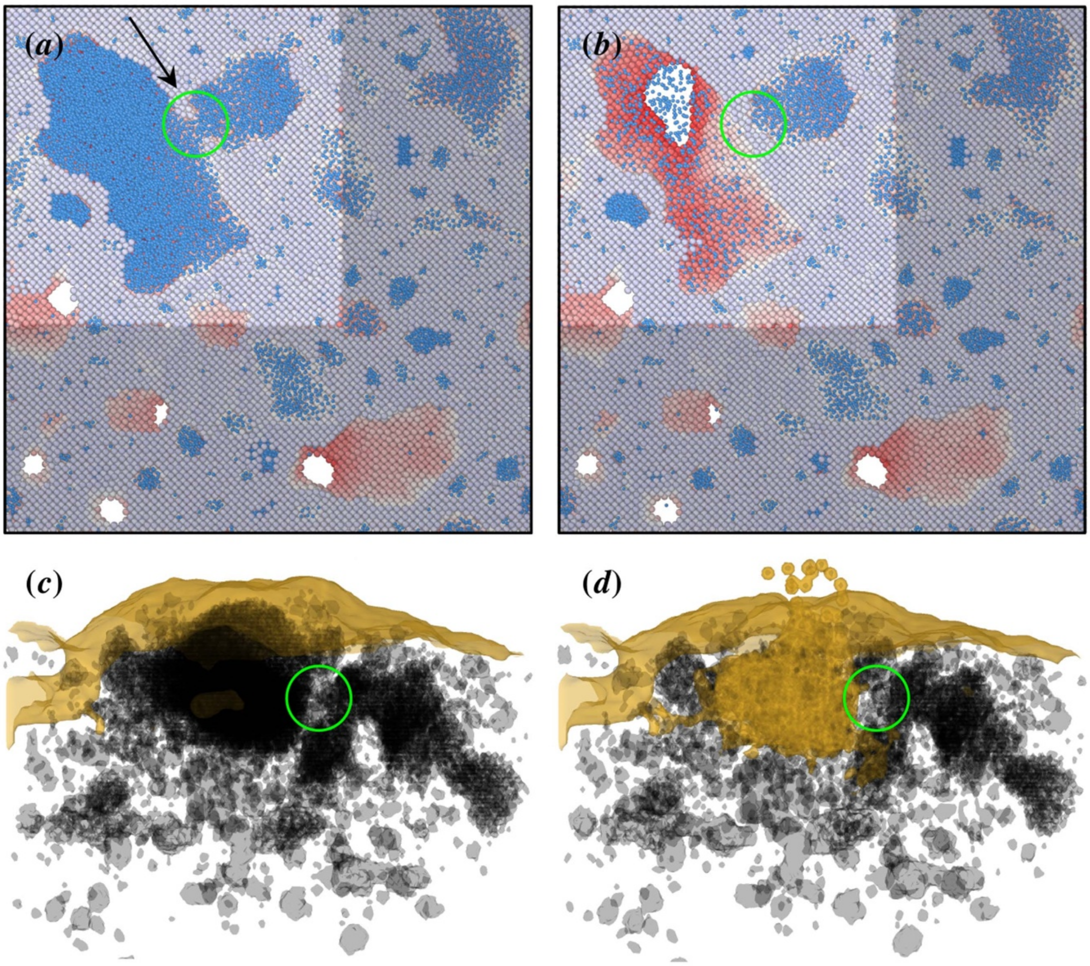

Figure 7. Snapshots of a large bubble connected to another large bubble shortly before and after the larger bubble bursts, leaving the smaller bubble intact. (*a*) View from the bottom (in the direction of the plasma) of a cross-section of the system in figure 5 with the same color scheme at $t = 122.906$ ns (corresponding to a fluence of 6.066×10^{20} m^{-2}) cut at a depth of 5 nm. (*b*) The same view at $t = 123.025$ ns (fluence of 6.072×10^{20} m^{-2}). (*c*) Side view of the system in (*a*) without the slice and excluding the shaded regions, viewed along the arrow in (*a*). (*d*) Similar side view of (*b*), without the shaded regions and without the slice, at the same camera position as in (*c*). The connection between the two large bubbles is circled.

Finally, the original article discussed the interconnected network of cavities that was present in these simulations. To give an idea of the extensive nature of these cavities, consider the crater seen venting helium atoms in the upper middle portion of figure 5(*i*). The bubble that creates this crater is at one time joined to the bubble that creates the crater in the upper left of figure 5(i) by a 'tunnel' roughly 1 nm in diameter. This tunnel is obscured in figure 5; a more obvious angle is shown in figure 7. Note that the atoms in figure 7 have been translated and wrapped back into the simulation box via periodic boundary conditions so as to center the bubbles in question in the upper left portion of the images. When the larger bubble bursts, the 'tunnel' that connects the two bubbles is pinched closed. This allows the smaller bubble to remain intact and almost unchanged while the larger bubble vents completely. Some time later, the smaller bubble bursts and leaves behind the deep, nearly-spherical cavity on the right-hand side of figure 5(ℓ). Six other bubbles then burst through this cavity and vent through the accompanying crater over the next 47.5 ns, at which point the crater seals up again. The cavity begins to refill immediately and bursts about 46 ns later, creating the bottom-most crater in Figure 5(q) (which was nearly healed over by the time the snapshot was taken).

3. Conclusions

The conclusions of the original paper are unaffected. In particular, we affirm our conclusion that bubbles can grow, be partially or completely filled in, refill, and burst again. We also conclude that it is possible for one bubble to burst and vent its helium to the plasma, sealing off connections to other bubbles nearby in the process because of changes in local stress caused by bursting. In general, the presence of craters, cavities, and other defects has a complicated relationship with helium bubbles and their tendencies to burst.

Acknowledgments

The authors thank Aidan Thompson (Sandia National Laboratories) for a helpful discussion regarding possible causes of this glitch.

This material is based upon work supported by the US Department of Energy, Office of Science, Office of Fusion Energy Sciences, and Office of Advanced Scientific Computing Research through the Scientific Discovery through Advanced Computing (SciDAC) project on Plasma-Surface Interactions at Oak Ridge National Laboratory, as well as subcontracts 4000135920 and 4000159698 through Oak Ridge National Laboratory and award numbers DE-SC0008875 and DE-SC0018421.

This work used computing resources at the National Energy Research Scientific Computing Center (NERSC), a DOE Office of Science User Facility supported by the Office of Science of the US Department of Energy under Contract No. DE-AC02-05CH11231. This research also used resources of the Argonne Leadership Computing Facility, which is a DOE Office of Science User Facility supported under Contract No. DE-AC02-06CH11357.

Oak Ridge National Laboratory is managed by UT–Battelle, LLC for the US Department of Energy under Contract No. DE-AC05-00OR22725.

ORCID iDs

Karl D. Hammond https://orcid.org/0000-0002-5424-8752

Dimitrios Maroudas https://orcid.org/0000-0001-9297-8839

Brian D. Wirth https://orcid.org/0000-0002-0395-0285

References

[1] Hammond K.D., Naeger I.V., Widanagamaachchi W., Lo L.T., Maroudas D. and Wirth B.D. 2019 *Nucl. Fusion* **59** 066035

[2] Hammond K.D., Blondel S., Hu L., Maroudas D. and Wirth B.D. 2018 *Acta Mater.* **144** 561–78

[3] Stukowski A. 2010 *Model. Simulat. Mater. Sci. Eng.* **18** 015012

[4] Sefta F., Hammond K.D., Juslin N. and Wirth B.D. 2013 *Nucl. Fusion* **53** 073015

[5] Doerner R.P., Nishijima D., Krasheninnikov S.I., Schwarz-Selinger T. and Zach M. 2018 *Nucl. Fusion* **58** 066005